

## A research on the statistical relationships between auroras and geinduced currents in power electric systems of the Russian Arctic

Vorobev, A.V.<sup>1</sup>  | Vorobeva, G.R.<sup>1</sup> 

1. Department of Informatics, Ufa University of Science and Technology, Ufa, Russia.

Corresponding Author E-mail: [geomagnet@list.ru](mailto:geomagnet@list.ru)

(Received: 21 July 2024, Revised: 22 Dec 2024, Accepted: 5 March 2025, Published online: 15 March 2025)

### Abstract

Confident progress in developing the Russian Federation's Arctic zone requires minimizing the negative impacts of space weather on electric power systems within the auroral oval. Some scientific studies propose methods for remote diagnostics of geinduced currents (GIC) levels. However, despite the high accuracy of these methods, their applicability remains uncertain, and they cannot be implemented in regions lacking a dense coverage of reliable geomagnetic data sources, such as the Taimyr and Gydan Peninsulas and northern Yakutia. This paper discusses an approach to the non-hardware-based assessment of GIC levels in high-latitude electric power systems. The proposed method is based on GIC observation data from the Kola-Karelian transit area, which includes power transmission lines and substations forming a single chain over 1,100 km in length. Its distinctive feature is the use of auroras as natural indicators of the space weather conditions for problem-oriented interpretation.

Using the example of the Vykhodnoy substation in the Northern Transit main power grid, it has been shown that the most probable (averaged over 30 minutes) GIC levels are 0.08 A, 0.23 A, and 0.68 A when auroras are observed to the north, at the zenith, and to the south, respectively. The probability of the average half-hour GIC level exceeding 2 A (when auroras are observed to the north, at the zenith, and to the south) is approximately 6%, 10%, and 15%, respectively. Finally, promising modernization methods and the applicability limits of the proposed approach are discussed.

**Keywords:** Geinduced currents, Auroras, Geomagnetic variations, Space weather, High-latitude power systems, Statistical models.

### 1. Introduction

As is well known, the auroral oval is a belt of intense luminosity caused by the entry of electrons from near-Earth space into the atmosphere. High-latitude infrastructure in this region faces the greatest risks from space weather affecting electric power systems. One of the most significant impacts of space weather on ground infrastructure during magnetic storms and substorms are geinduced currents (GIC). These currents are primarily induced in conductive structures such as pipelines, railways, and power transmission lines (Marshall et al., 2011; Vorobev et al., 2019).

High-latitude power transmission lines, often with complex geometry, can be considered global antennas that are electromagnetically coupled with the currents of the Earth's ionosphere. According to experts (Pirjola et al. 2003), during magnetic storms,

Geomagnetically Induced Currents (GIC) of up to 200–300 A can occur in grounded networks. These currents, with an intensity of several amperes, can push certain types of transformers out of their linear mode, leading to emergencies.

For example, on March 13, 1989, a magnetic storm caused the failure of power transformers and a cascade blackout of Power Transmission Lines (PTL) for more than nine hours in the province of Quebec in Canada (Kataoka & Ngwira, 2016). In November 2001, the geomagnetic activity (GMA) caused two shutdowns in the Olenegorsk-Monchegorsk power line (330 kV) at the unified energy system of northwestern Russia, and so many electricity consumers were disconnected. In October 2003, GMA also caused a 20–50-minute power outage in the Malmö power grid in southern Sweden. At the

Cite this article: Vorobev, A.V., & Vorobeva, G.R. (2025). A research on the statistical relationships between auroras and geinduced currents in power electric systems of the Russian Arctic. *Journal of the Earth and Space Physics*, 50(4), 219-228. DOI: <http://doi.org/10.22059/jesphys.2025.385178.1007644>

E-mail: (1) [gulnara.vorobeva@gmail.com](mailto:gulnara.vorobeva@gmail.com)



Publisher: University of Tehran Press.

DOI: <http://doi.org/10.22059/jesphys.2025.385178.1007644>

Print ISSN: 2538-371X  
Online ISSN: 2538-3906

same moment, there was a "false trip" of a relay at the Olenegorsk substation, which was detected at the very beginning of a magnetic storm (Radasky et al., 2019; Tanskanen, 2009). According to a report by Zurich Insurance Group, in the United States alone, electrical equipment failures during magnetic storms from 2005 to 2015 resulted in insurance payments exceeding \$1.9 billion (Dobbins & Schriever, 2015). Furthermore, (Pilipenko, 2021; Pilipenko et al., 2023) noted that the current interference after strong magnetic storms usually causes synchronous anomalies in railway automation systems on the northern branches of the Oktyabrskaya and Severnaya railways, located beyond the Arctic Circle.

The problem has become even more serious because, during extreme GMA, the shift of the auroral oval in the equatorial direction makes these risks relevant for electric power systems operating at mid- and even near-low latitudes (Pratscher et al., 2024).

The relationships between geomagnetic variations (GMV) and the GIC level established by Vorobev et al. (2019, 2022a) provide the ability for diagnostics of current interference when appropriate sources of geomagnetic data are available, with an accuracy depending on their quantity and quality. For example, according to Vorobev et al. (2022b), the GIC level at the Vykhodnoy station (VKH) averaged over 15 minutes, can be estimated with a root-mean-square error of  $\sim 0.122 \text{ A}^2$ .

Despite the high accuracy of the method, the limits of its applicability, within which the mentioned dependence maintains its linear nature, remain unclear. However, a more significant issue with this approach is that it cannot be applied to regions lacking dense coverage by reliable geomagnetic data sources, such as the Taimyr Peninsula, the Gydan Peninsula, and the northern regions of the Sakha Republic (Yakutia), among others. This situation is typical for most of the Arctic Zone of the Russian Federation (AZRF) and practically excludes the possibility of prompt diagnostics of the high-latitude electric power systems response to changes in the upper ionosphere state. In this area of the Arctic zone, the auroras remain practically the only publicly available indicator of space weather. Thus, the research is concerned with detecting the statistical and correlational relationships

between auroras and GIC. These relationships can provide the possibility of non-instrumental assessment of the GIC in conditions of data deficiency, which is typical for the Asian part of the Arctic region.

## 2. Experimental data

The Lovozero Observatory (LOZ) is part of the Polar Geophysical Institute (PGI) and is one of the few stations in the Russian Federation that continuously conducts long-term observations and records of auroras, magnetic field variations, and other high-latitude geophysical effects caused by processes in the magnetosphere, ionosphere, and atmosphere of the Earth. The observatory is the main source of aurora observation data. Auroral data in the vicinity of the LOZ observatory (Figure 1) have been analyzed over a period of more than 10 years (from October 10, 2011, to December 31, 2021). Corresponding to the highest quality results of synchronous observations of the sky and the GIC level in the subregion bounded by  $67.97^\circ \text{ N}$ ,  $35.02^\circ \text{ E}$  (Lovozero village, Murmansk region, Russia) and  $68.83^\circ \text{ N}$ ,  $33.08^\circ \text{ E}$  (Vykhodnoy transformer substation (VKH), Murmansk region, Russia).

Since 2009, the results of aurora observations have been published by PGI in the form of quarterly sets of ASCAPLOTS (All Sky CAmera PLOTs) (Fukunishi & Ayukawa, 1972; PGI Geophysical data) (Figure 2). These results are available at: [http://pgia.ru/lang/ru/archive\\_pgi](http://pgia.ru/lang/ru/archive_pgi).

The ASCAPLOTS format has remained unchanged since the 1970s and is ineffective for the intelligent analysis of large volumes of data (Vorobev et al., 2023a). In this regard, the authors have proposed an algorithm for transforming ASCAPLOTS into electronic tables (Vorobev et al., 2023b). The records here were synchronized with the GIC values recorded at the VKH station (Figure 1). The data have been made available because in 2011, the Kola Science Center of the Russian Academy of Sciences, in collaboration with PGI, and with the support of the Federal Grid Company of Unified Energy System (FGC UES), founded a regional system for monitoring currents in transformer neutrals. The system accumulated a significant amount of data on the impact of GMA on the main electrical network with a length of over 800 km (Barannik et al., 2012). In 2022, a database

of GIC measurements in the neutrals of autotransformers at three substations (Vykhodnoy, Louhi, Kondopoga) within the 330 kV Northern Transit main electrical network for the period 2011–2022 was published (Certificate of the Russian Federation on state registration of the database No. 2022623220 “Geinduced currents in the Northern Transit main electrical network”, <http://gic.en51.ru>) (Selivanov et al., 2023). Thus, as a result of digitizing 1921 ASCAPLOTS for 2011–2021, 92,208 episodes of 30-minute synchronous sky observations in the vicinity of the LOZ observatory and the GIC level at the VKH station were obtained (Table 1).

$$J_{VKHn} = \frac{1}{N} \sum_{m=n}^{n+\Delta t_1/\Delta t_2} |J'_{VKH}|_m \quad (1)$$

where  $\Delta t_1$  is a discretization step of optical observations of auroras (ASCAPLOTS) with  $\Delta t_1= 30$  min,  $\Delta t_2$  is the discretization step for GIC  $\Delta t_2=0.5$  s,  $J'_{VKH}$  represents the GIC data published by PGI.

As an example, the time diagram of synchronous registration of the GIC at the VKH substation and auroras by the LOZ observatory as of December 14, 2013 is shown in Figure 3. According to the time diagram, the periods of auroras presence correspond to the time intervals during which significant variations occur in the GIC. At the same time, the existence of auroras in the southern part of the sky correlates with the occurrence of extreme GIC values.

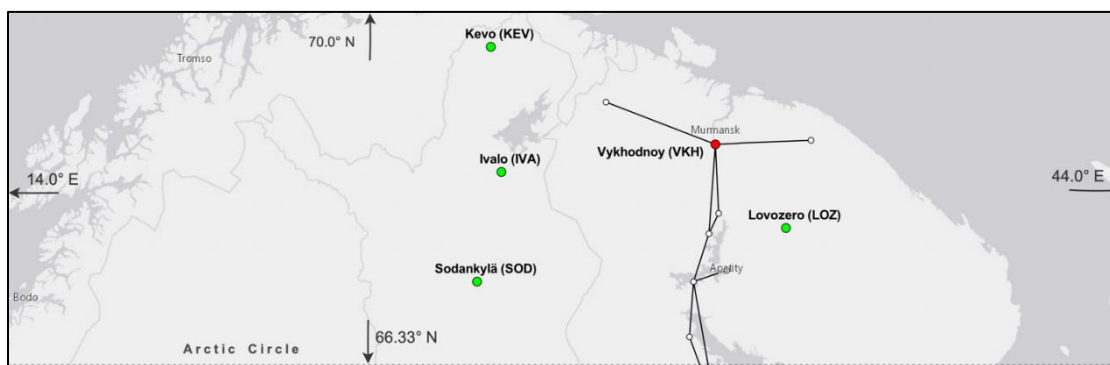


**Figure 1.** The geography of daily the Northern Transit main power grid is represented by a solid black line, including the Vykhodnoy transformer substation, which is marked with a red marker. Green markers correspond to nearby magnetic stations, with the Lovozero (LOZ) magnetic station, which belongs to the Murmansk Department for Hydrometeorology and Environmental Monitoring, and the observatory that is part of the Polar Geophysical Institute. These two facilities are spatially indistinguishable in the figure.

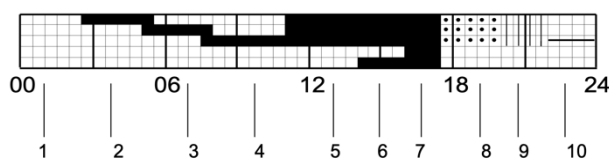


**Figure 2.** An example of data presentation in the ASCAPLOTS format: 1 – No aurora observed; 2 – Aurora in the northern region; 3 – Aurora at zenith; 4 – Aurora in the southern region; 5 – Aurora at zenith, northern and southern regions; 6 – Moderate aurora at zenith, in addition, aurora is present in the northern and southern regions; 7 – Strong aurora at zenith, in addition, aurora is present in the northern and southern regions; 8 – Partial cloudiness; 9 – Solid cloudiness; 10 – No registration was carried out.

**Table 1.** Fragment of dataset from synchronous observation of polar auroras and GIC.

No.	UTC	$J_{VKHn}$ , A	Auroras in the north	Auroras at the zenith	Auroras at the south
...	...	...	...	...	...
12191	2013-12-14 18:00	1.415	1	1	2
12192	2013-12-14 18:30	8.226	1	1	1
12193	2013-12-14 19:00	8.179	1	1	2
12194	2013-12-14 19:30	2.878	1	1	2
...	...	...	...	...	...

Note:  $J_{VKHn}$  is the value of the GIC, determined in accordance with expression (1); 0 – no auroras; 1 – auroras present; 2 – cloudiness.

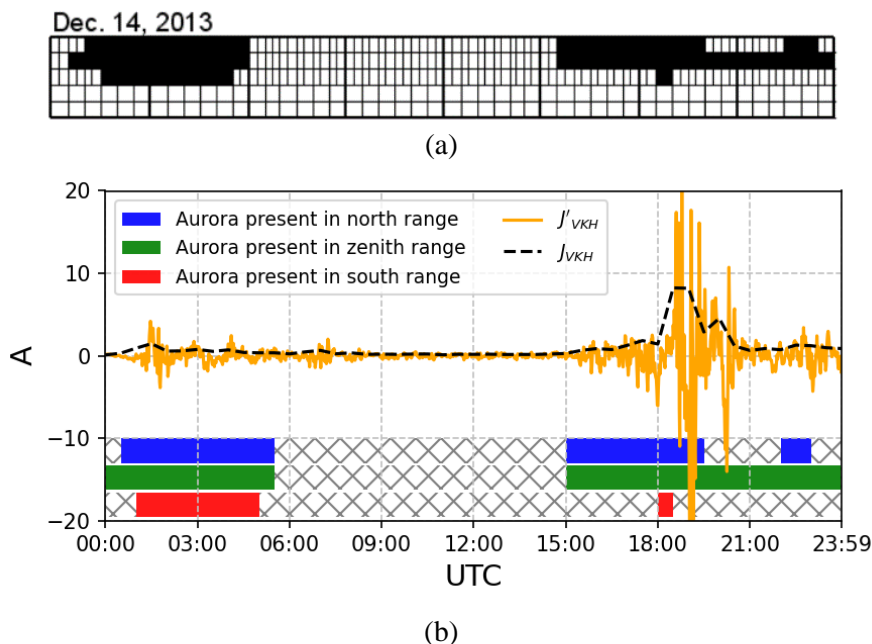


**Figure 3.** An example of comparing the aurora observation area at the LOZ station and the GIC level at the VKH station for December 14, 2013. ASCAPLOTS (a) is presented from the PGI archive [PGI Geophysical data].

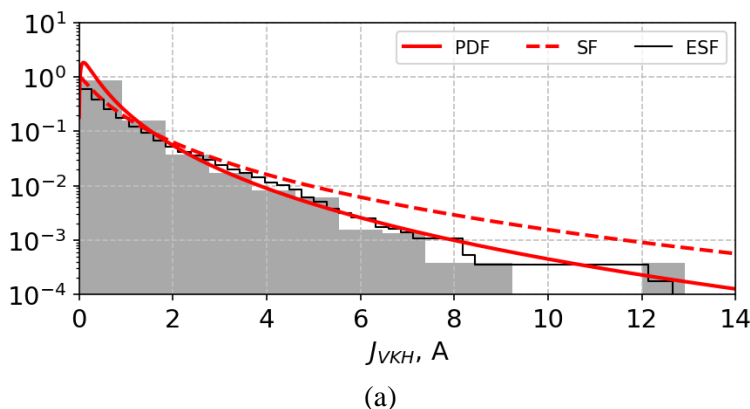
**3. Correlation-statistical relationships between GIC and aurora observation area**

The distribution type of a random variable is mainly determined by the physical mechanisms of the analyzed process. Let's consider an observation of the cumulative effect of many random, weakly interdependent variables. Each variable makes its own relative contribution to the total value, forming a normal distribution. Additionally, in a closed system, the energy of its components is distributed according to an exponential law or the Laplace law. A random multiplicative combination of several parameters leads to a lognormal distribution, and so on. Particular attention should be given to the heavy tails of the distribution, as their presence suggests that the dispersion of the random variable is determined predominantly by rare, high-intensity deviations rather than frequent, small ones.

The distribution pattern of  $J_{VKH}$  values with simultaneous observation of auroras in different areas of the sky (Figure 4) best corresponds to the lognormal law (Equation 2) (Eckhard et al., 2001). This can be confirmed by the results of the Kolmogorov-Smirnov test (Dimitrova et al., 2020). The result is consistent with the previously obtained findings (Vorobev et al., 2019; Vorobev & Pilipenko, 2021; Vorobev et al., 2022) and does not contradict the research published by PGI (Barannik et al., 2012; PGI Geophysical Data, 2013).

$$PDF(x, s) = \frac{1}{sx\sqrt{2\pi}} \exp\left(-\frac{\log^2 x}{2s^2}\right) \quad (2)$$

where PDF is the probability density function;  $s$  is the shape parameter (also known as the form parameter, which is a kind of numerical parameter in a parametric family of probability distributions) (Everitt, 2002).



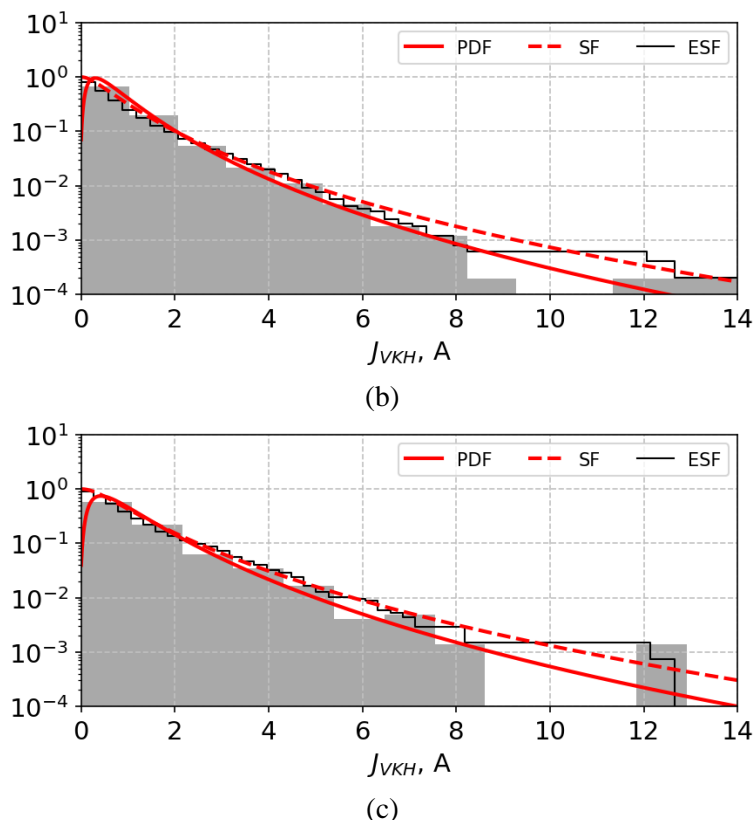


**Figure 4.** Statistics of the GIC when observing auroras in the north (a), at the zenith (b) and in the south (c). The gray solid and dashed lines correspond to the probability density functions (PDF) and survival function of the lognormal distribution law ( $SF=1-CDF$ , where CDF is the cumulative distribution function), respectively. The black solid line is the empirical survival function ( $ESF=1-ECDF$ , where ECDF is the empirical cumulative distribution function) (Dekking, 2005)

An analysis of the distributions (Figure 4) proved that the most probable  $J_{VKH}$  values when observing auroras in the north, at the zenith, and in the south are 0.08 A, 0.23 A, and 0.68 A, respectively (Figure 5, b). The result is explained by the expansion of the auroral oval during periods of strong GMA. Additionally, the result provides data for predicting the level of currents induced in high-latitude power transmission lines as a function of the region of auroral manifestation in the optical range. Further, it can be concluded that when observing auroras in the north, the probability that the average half-hourly GIC level in the electric power system will exceed, for example, 2 A, is ~6%, while during auroras at the zenith and in the south, the probability of exceeding a similar GIC level is ~10% and ~15%, respectively (Figure 5, b). The probability that  $J_{VKH}$  will exceed 10 A during the auroral period in the south is 0.15%, versus 0.06% and 0.04% when observing aurora at the zenith and in the north,

respectively.

In the same way, the geometry of the distribution tail associated with the frequency of extreme GIC occurrence was shaped (Figures 4–5). For example, the statistics of GIC during auroras in the south (Figure 4, c) have minimum asymmetry and excess values, which characterize the thickest tail and, consequently, the maximum frequency of extreme GIC occurrence during these periods. Along with this, during periods of observation of weak, diffuse auroras in the north, or their absence, the GIC statistics are characterized by the highest asymmetry and excess values. This suggests that  $J_{VKH}$  values are maximally concentrated in the lower range and have the least uncertainty (Figure 5, a). Furthermore, the analysis of Figures 4–5 indicates that the occurrence of extreme GIC practically determines the presence of polar auroras; however, the observation of auroras does not necessarily guarantee the occurrence of extreme GIC.

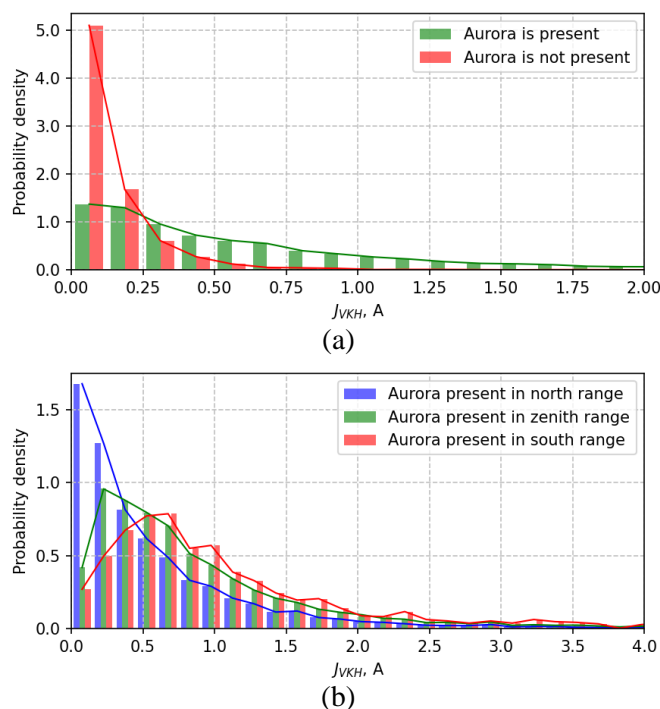


**Figure 5.** Histogram of the probability density distribution of GIC values in the presence or absence of auroras (a) and when differentiated by sky regions (b). The width of the histogram intervals in this case is determined according to the rule:  $h_n = 3.49sn^{-1/3}$ , where  $n$  is the sample size,  $s$  is the standard deviation (Scott, 1979) and corresponds to  $\sim 0.15$  A.

The correlation analysis of  $J_{VKH}$  values with the aurora manifestation area reveals a connection between current interference in high-latitude power systems and the regions where auroras are observed. During periods of aurora observation at the zenith, the Spearman rank correlation coefficient is determined at a level of  $\sim 0.7$ , which is twice higher than cases of aurora occurrence in the north or south. This result suggests that GIC is nonlinearly related to the GMA level and strongly depends on the location of the affected object relative to the boundaries of the auroral oval.

#### 4. Correlation-statistical model of the GIC level

It is necessary to consider an approach to diagnosing GIC based on aurora observation data, using Bayes' theorem.:

$$P(A|B) = \frac{P(B|A)P(A)}{P(B)} \quad (3)$$

here:

$P(A)$  is the prior probability of hypothesis  $A$  or the prior distribution;

$P(A|B)$  is the probability of hypothesis  $A$  given the occurrence of event  $B$  (posterior probability);

$P(B|A)$  is the probability of event  $B$  given the truth of hypothesis  $A$ ;

$P(B)$  is the total probability of event  $B$ , determined in accordance with expression (4).

$$P(B) = \sum_{i=1}^N P(B|A_i)P(A_i) \quad (4)$$

where the probabilities under the sum sign are known or can be estimated experimentally.

In the context of the problem being solved, we have the following:

$$P(A|B) = \frac{P(B|A)P(A)}{P(B|A)P(A) + P(B|\sim A)P(\sim A)} \quad (5)$$

where

$P(A|B)$  is the probability that, when observing auroras in a given region,  $J_{VKH} \geq J_0$ , where  $J_0 = \text{const}$  is some given value of the GIC;

$P(B|A)$  is the probability of observing auroras in a given region when  $J_{VKH} \geq J_0$ ;

$P(A)$  and  $P(\sim A)$  are the probabilities that  $J_{VKH} \geq J_0$  and  $J_{VKH} < J_0$ , respectively;

$P(B|\sim A)$  is the probability of observing auroras in a given region when  $J_{VKH} < J_0$ .

Thus, the *a posteriori* probability that the GIC level at the JVKH station will exceed 2 A when auroras are observed in the north is 5.78%, while the probability of exceeding this value when there are auroras at the zenith and in the south is 10.04% and 14.93%, respectively (Figure 6). In the absence of auroras, the probability of  $J_{VKH}$  reaching a similar level does not exceed 0.26%, and the probability of exceeding 3 A is 0.00%.

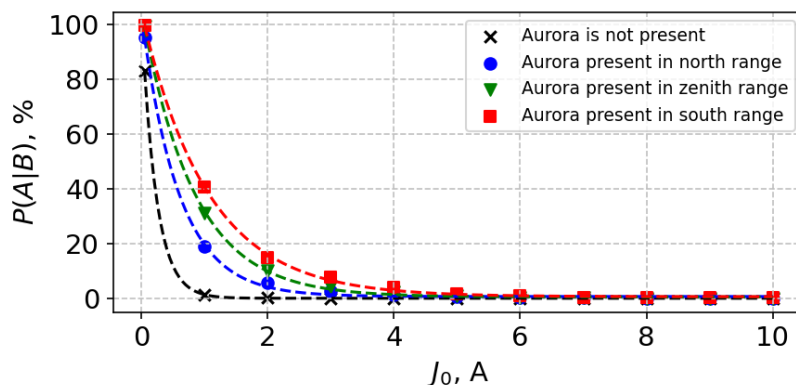


**Figure 6.** The a posteriori probability of exceeding the GIC level  $J_0$  at the VKH station with simultaneous observation of auroras in different areas of the sky. Markers indicate empirical values; dotted lines indicate approximation of empirical values by expression (6).

The dependence of the probability of exceeding the GIC level  $J_0$  follows an exponential character (Figure 6), varies based on the region of manifestation relative to the object of influence of auroras, and has a discrepancy not exceeding  $10^{-8}$  of the measured value:

$$P(A|B) \approx P(J_0) = a \cdot \exp(b \cdot J_0) + c \quad (6)$$

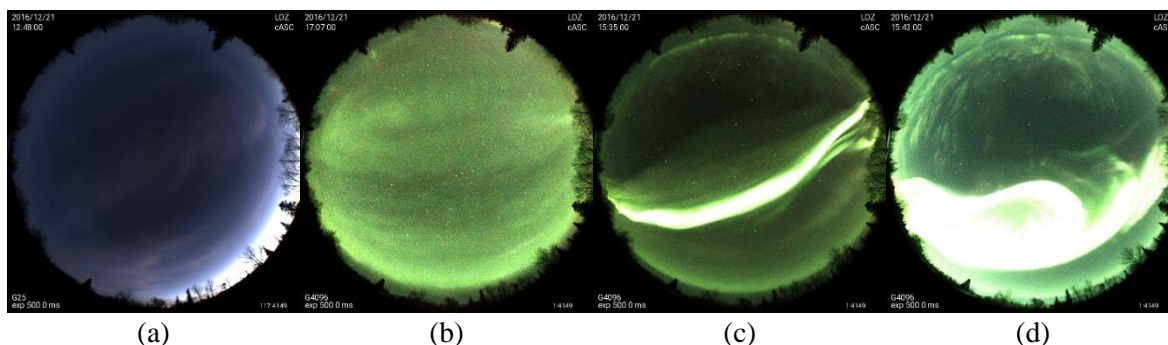
where  $a = 102.87$  for cases of absence of auroras,  $a = 102.68, 104.69, 103.60$  for cases of aurora observation in the north, at the zenith, and in the south, respectively; similarly,  $b = -4.34, -1.69, -1.21, -0.95$ , and  $c = 0.04, 0.68, 0.53, 0.62$  for cases of absence of auroras and their observation in the north, at the zenith, and in the south, respectively.

### 5. Discussion of results

The obtained results demonstrate that the presence of auroras is a necessary but insufficient condition for the existence of extreme GIC in high-latitude power systems (Wintoft et al., 2015). Furthermore, the

analysis of the examined sub-region has revealed a correlation between the extent of auroral observation and current disturbances in high-latitude electrical networks. Under such conditions, the obtained result may function as a natural indicator for assessing the potential level of Geomagnetically Induced Currents (GIC) in polar power transmission lines.

Preliminary investigations have identified a correlation between the GIC level and the intensity and structure of auroral phenomena (Figure 7). The experiments conducted to validate these results were based on data from the synchronous registration of sky conditions and GIC on December 21, 2016. Thus, during periods without auroras (12:48 UT), the average minute GIC level was 0.1 A; for diffuse auroras (17:07 UT), it was 0.7 A; and for intense auroras of the ‘arc’ (15:35 UT) and ‘vortex’ (15:43 UT) types, the levels were 1.34 A and 13.06 A, respectively (Vorobev et al., 2024).



**Figures 7.** The sky state recorded by the All-sky camera (Sigernes et al., 2014) of the LOZ observatory at different times of the day on December 21, 2016, included: a – no auroras; b – diffuse auroras; c – arc-type auroras; d – vortex-type auroras.

Thus, it is necessary to assume that the operational identification of the intensity and structure of auroras (for example, ‘diffuse, arc, or vortex’) can significantly enhance the efficiency of using natural indicators of space weather to evaluate its impact on high-latitude infrastructure objects.

In conclusion, it should be noted that since this research primarily employed statistical methods, the numerical values of some of the results obtained are merely estimates and may vary when compared with other experimental data. However, the relationships among them are expected to remain consistent

## 6. Conclusion

There are known risks of a decline in the technical infrastructure safety level within the auroral oval area, associated with the effects of space weather on power electric systems. However, the existing monitoring systems for the prompt diagnostics of extreme Geomagnetically Induced Currents (GIC) in the power systems of the Russian Arctic are ineffective. In this regard, the only universally

accessible indicator of space weather conditions remains the auroras. The interpretation of these auroras can be utilized to reduce the level of situational unawareness regarding the risks of failures in polar power distribution and navigation systems, communication systems, and high-latitude railway infrastructure facilities (Figure 8).

The authors processed approximately 2,000 ASCAPLOTS over a more-than-10-year observation period, including 92,208 episodes of 30-minute sky observations in the vicinity of the LOZ station. The results proved that the most probable GIC level at the VKH station when registering auroras in the north, at the zenith, and in the south is 0.08 A, 0.23 A, and 0.68 A, respectively. At the same time, the *a posteriori* probability during auroras in the north that  $J_{VKH}$  will exceed 2 A is 5.78%. The probability of exceeding this value during auroras at the zenith and in the south is 10.04% and 14.93%, respectively. In the absence of auroras, the probability of reaching  $J_{VKH}$  a similar level does not exceed 0.26%, and the probability of exceeding 3 A is 0.

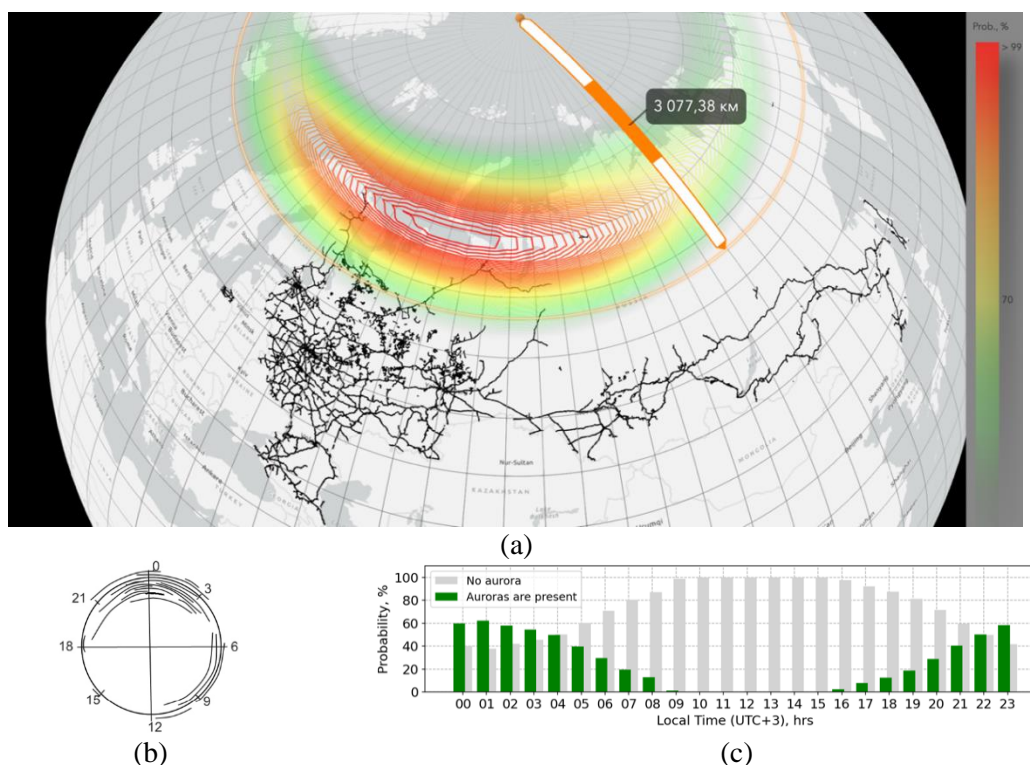


**Figure 8.** On the possibility of diagnostics and forecasting for the probability of failures of high-latitude railway automation systems based on natural indicators of the state of space weather: a - An example of visualization of the relative position of a short-term forecast of the probability of visibility of auroras and the main railway lines of the Russian Federation during a magnetic storm with an auroral index  $AE = 1450$  nT. The forecast is based on data from <https://aurora-forecast.ru> as of 2022-02-17, 18:30 UT (Vorobev et al., 2022); b - Distribution of railway automation anomalies on the Northern Railway relative to local time during periods of strong magnetic storms in 1989 and 2000-2005 (Eroshenko et al., 2010); c - Diurnal variations in the probability of observing auroras in the vicinity of the LOZ station.

It has been proven that the probability of exceeding a certain level of Geomagnetically Induced Currents (GIC) decreases exponentially with an increase in this level. The value depends on the region of aurora manifestation and can be well approximated by an expression  $P(A|B) \approx P(J_0) = a \cdot \exp(b \cdot J_0) + c$ , where  $P(A|B)$  is the probability of exceeding the GIC level  $J_0$  when observing auroras in a given region;  $a$ ,  $b$ , and  $c$  are coefficients determined empirically.

Moreover, the proposed approach is important for assessing the probability of failures in high-latitude railway automation systems, as well as for estimating the possible additional error of magnetic inclinometers, which are widely used in directional drilling in the Arctic Zone of the Russian Federation (Soloviev et al., 2022). A limitation of the proposed approach is that ground-based registration of auroras in the night sky at high latitudes is possible only for up to seven months a year, provided that the meteorological conditions are favorable.

## 7. Acknowledgments

The authors thank the reviewers, whose comments significantly improved the quality of the paper.

The authors also express their gratitude to the Polar Geophysical Institute (PGI) for the provided data on the observation of the auroras by the Lovozero Observatory, as well as to the PGI and the Center for Physical and Technical Problems of Northern Energy of the Kola Science Center of the Russian Academy of Sciences for the data on geinduced currents recorded at the Vykhodnoy station.

The research was supported by the Russian Science Foundation grant No. 25-21-00143, <https://rscf.ru/project/25-21-00143/>.

## References

- Barannik, M. B., Danilin, A. N., & Kat'kalov, Yu. V. (2012). A system for recording geomagnetically induced currents in neutrals of power autotransformers. *Instruments and Experimental Techniques*, 55(1), 110–115. <https://doi.org/10.1134/S0020441211060121>
- Dimitrova, D. S., Kaishev, V. K., & Tan, S. (2020). Computing the Kolmogorov-Smirnov distribution when the underlying CDF is purely discrete, mixed, or continuous. *Journal of Statistical Software*, 95(10), 1–42. <https://doi.org/10.18637/jss.v095.i10>
- Dobbins, R. W., & Schriiver, K. (2015). *Electrical claims and space weather: Measuring the visible effects of an invisible force*. <https://static1.squarespace.com/static/57bc8a4a414fb50147550a88/t/57d84e4d1b631b96124f3c69/1473793614089/2015+Zurich-Electrical+Claims+and+Space+Weather.pdf>
- Eckhard, L., Werner, A. S., & Markus, A. (2001). Log-normal distributions across the sciences: Keys and clues. *BioScience*, 51(5), 341–352.
- Eroshenko, E. A., Belov, A. V., Boteler, D., Gaidash, S. P., Lobkov, S. L., Pirjola, R., & Trichtchenko, L. (2010). Effects of strong geomagnetic storms on Northern railways in Russia. *Advances in Space Research*, 46(9), 1102–1110. <https://doi.org/10.1016/j.asr.2010.05.017>
- Everitt, B. S. (2002). *Cambridge dictionary of statistics* (2nd ed.). Cambridge University Press.
- Fukunishi, H., & Ayukawa, M. (1972). Auroral observations at Syowa Station, 1970-1971. *Reports of the Japanese Antarctic Research Expedition*, 36–68.
- Kataoka, R., & Ngwira, C. (2016). Extreme geomagnetically induced currents. *Progress in Earth and Planetary Science*, 3, 23.
- Marshall, R. A., Smith, E. A., Francis, M. J., Waters, C. L., & Sciffer, M. D. (2011). A preliminary risk assessment of the Australian region power network to space weather. *Space Weather*, 9, S10004. <https://doi.org/10.1029/2011SW000685>
- PGI Geophysical data. (2013). *January, February, March 2013* (V. Vorobjev, Ed.). PGI KSC RAS.
- Pilipenko, V. A. (2021). Space weather impact on ground-based technological systems. *Solar-Terrestrial Physics*, 3, 72–110. <https://doi.org/10.12737/szf-73202106>
- Pilipenko, V. A., Chernikov, A. A., Soloviev, A. A., Yagova, N. V., Sakharov, Ya. A., Kostarev, D. V., Kozyreva, O. V., Vorobev, A. V., & Belov, A. V. (2023). Influence of space weather on the reliability of the transport system

- functioning at high latitudes. *Russian Journal of Earth Sciences*, 23, ES2008. <https://doi.org/10.2205/2023ES000824>
- Pirjola, R., Pulkkinen, A., & Viljanen, A. (2003). Studies of space weather effects on the Finnish natural gas pipeline and on the Finnish high-voltage power system. *Advances in Space Research*, 31(4), 795–805. [https://doi.org/10.1016/S0273-1177\(02\)00781-0](https://doi.org/10.1016/S0273-1177(02)00781-0)
- Pratscher, K. M., Ingham, M., Mac Manus, D. H., Kruglyakov, M., Heise, W., & Rodger, C. J. (2024). Modeling GIC in the southern South Island of Aotearoa New Zealand using magnetotelluric data. *Space Weather*, 22, e2024SW003907. <https://doi.org/10.1029/2024SW003907>
- Radasky, W., Emin, Z., & Adams, R. (2019). *CIGRE TB 780: Understanding of geomagnetic storm environment for high voltage power grids*. Technical report.
- Scott, D. W. (1979). On optimal and data-based histograms. *Biometrika*, 66(3), 605–610. <https://doi.org/10.1093/biomet/66.3.605>
- Selivanov, V. N., Aksenovich, T. V., Bilin, V. A., Kolobov, V. V., & Sakharov, Y. A. (2023). Database of geomagnetically induced currents in the main transmission line “Northern Transit”. *Solar-Terrestrial Physics*, 3, 100–110. <https://doi.org/10.12737/szf-93202311>
- Sigernes, F., Holmen, S. E., & Biles, D. (2014). Auroral all-sky camera calibration. *Geoscientific Instrumentation, Methods and Data Systems*, 3, 241–245. <https://doi.org/10.5194/gi-3-241-2014>
- Soloviev, A. A., Sidorov, R. V., & Oshchenko, A. A. (2022). On the need for accurate monitoring of the geomagnetic field during directional drilling in the Russian Arctic. *Izvestiya, Physics of the Solid Earth*, 58, 420–434. <https://doi.org/10.1134/S1069351322020124>
- Tanskanen, E. I. (2009). A comprehensive high-throughput analysis of substorms observed by IMAGE magnetometer network: Years 1993–2003 examined. *Journal of Geophysical Research*, 114, A05204. <https://doi.org/10.1029/2008JA013682>
- Vorobev, A. V., & Pilipenko, V. A. (2021). Geomagnetic data recovery approach based on the concept of digital twins. *Solar-Terrestrial Physics*, 2, 53–62. <https://doi.org/10.12737/szf-72202105>
- Vorobev, A. V., Lapin, A. N., & Vorobeva, G. R. (2023). Software for automated recognition and digitization of archive data of aurora optical observations. *Informatics and Automation*, 22(5), 1177–1206. <https://doi.org/10.15622/ia.22.5.8>
- Vorobev, A. V., Lapin, A. N., Soloviev, A. A., & Vorobeva, G. R. (2024). An approach to interpreting natural indicators of the state of space weather to assess the effects of its impact on high-latitude power systems. *Physics of the Solid Earth*, 4, 100–110. <https://doi.org/10.31857/S0002333724040071>
- Vorobev, A. V., Pilipenko, V. A., Sakharov, Y. A., & Selivanov, V. N. (2019). Statistical relationships between variations of the geomagnetic field, auroral electrojet, and geomagnetically induced currents. *Solar-Terrestrial Physics*, 1, 48–58. <https://doi.org/10.12737/szf-51201905>
- Vorobev, A. V., Soloviev, A. A., Pilipenko, V. A., & Vorobeva, G. R. (2022). Interactive computer model for aurora forecast and analysis. *Solar-Terrestrial Physics*, 2, 93–100. <https://doi.org/10.12737/szf-82202213>
- Vorobev, A. V., Soloviev, A. A., Pilipenko, V. A., Vorobeva, G. R., Gainetdinova, A. A., Lapin, A. N., Belakhovsky, V. B., & Roldugin, A. V. (2023). Local diagnostics of aurora presence based on intelligent analysis of geomagnetic data. *Solar-Terrestrial Physics*, 9(2), 22–30. <https://doi.org/10.12737/stp-92202303>
- Vorobev, A., Soloviev, A., Pilipenko, V., Vorobeva, G., & Sakharov, Y. (2022). An approach to diagnostics of geomagnetically induced currents based on ground magnetometers data. *Applied Sciences*, 12(3), 1522. <https://doi.org/10.3390/app12031522>
- Wintoft, P., Wik, M., & Viljanen, A. (2015). Solar wind-driven empirical forecast models of the time derivative of the ground magnetic field. *Journal of Space Weather and Space Climate*, 5, A7. <https://doi.org/10.1051/swsc/2015008>